MOLECULAR AND CELLULAR BIOLOGY, Oct. 2007, p. 6706–6717 Vol. 27, No. 19
0270-7306/07/$08.00+0 doi:10.1128/MCB.01225-07

Deletion of Shp2 in the Brain Leads to Defective Proliferation and Differentiation in Neural Stem Cells and Early Postnatal Lethality▽†

Yuehai Ke,[1]‡ Eric E. Zhang,[1,2]‡ Kazuki Hagihara,[1]‡ Dongmei Wu,[1] Yuhong Pang,[1] Rüdiger Klein,[3] Tom Curran,[4] Barbara Ranscht,[1] and Gen-Sheng Feng[1,2]*

Burnham Institute for Medical Research, 10901 N. Torrey Pines Rd., La Jolla, California 92037[1]; Molecular Pathology Graduate Program, University of California—San Diego, La Jolla, California 92093[2]; Department of Molecular Neurobiology, Max Planck Institute of Neurobiology, 82152 Martinsried, Germany[3]; and Children's Hospital of Philadelphia, 517 Abramson Research Center, 3615 Civic Center Boulevard, Philadelphia, Pennsylvania 19104-4318[4]

Received 9 July 2007/Accepted 16 July 2007

The intracellular signaling controlling neural stem/progenitor cell (NSC) self-renewal and neuronal/glial differentiation is not fully understood. We show here that Shp2, an introcellular tyrosine phosphatase with two SH2 domains, plays a critical role in NSC activities. Conditional deletion of Shp2 in neural progenitor cells mediated by Nestin-Cre resulted in early postnatal lethality, impaired corticogenesis, and reduced proliferation of progenitor cells in the ventricular zone. In vitro analyses suggest that Shp2 mediates basic fibroblast growth factor signals in stimulating self-renewing proliferation of NSCs, partly through control of Bmi-1 expression. Furthermore, Shp2 regulates cell fate decisions, by promoting neurogenesis while suppressing astrogliogenesis, through reciprocal regulation of the Erk and Stat3 signaling pathways. Together, these results identify Shp2 as a critical signaling molecule in coordinated regulation of progenitor cell proliferation and neuronal/astroglial cell differentiation.

Neural stem/progenitor cells (NSCs) are clonogenic cells capable of self-renewal and also generating all neuronal and glial cell lineages. Environmental cues, including growth factors and components of the extracellular matrix, play critical roles controlling self-renewal and maintenance of NSCs and also their differentiation. Epidermal growth factor (EGF) and basic fibroblast growth factor (bFGF) have been shown to induce neural fate specification in embryonic stem cells (ESCs) and potently stimulate the self-renewal capacity of NSCs in vivo and in vitro (12, 35, 37). Transcription factors, such as the polycomb family transcriptional repressor Bmi-1, are required for NSC self-renewal (22).

There is a gap in our understanding of the molecular link between cytoplasmic signals initiated by growth factors and the control of NSC activities. Signaling through the Mek-Erk pathway regulating the C/EBP family of transcription factors was shown to promote cortical neurogenesis from NSCs, while suppressing gliogenesis (20). In contrast, activation of the Jak/Stat pathway promotes gliogenesis with concomitant suppression of neurogenesis (2, 15).

Shp2, an Src-homology 2 domain (SH2)-containing tyrosine phosphatase, is a widely expressed intracellular enzyme that regulates signaling events downstream of several growth factor/cytokine receptors in various cell types (8, 18). In previous experiments, we demonstrated a stringent requirement for Shp2 in hematopoiesis, using in vitro ESC differentiation assays and chimeric animal analysis (28–30). Shp2-deficient erythroid, myeloid, or lymphoid progenitor cells are barely detectable in fetal liver, bone marrow, thymus, or spleen in the chimeric animals derived from aggregation of homozygous Shp2 mutant ESCs and wild-type embryos. However, it is interesting to note that Shp2-deficient cells were detected in many other nonhematopoietic tissues and organs, including the brain (29). This observation suggests that Shp2 ablation does not completely block neural development from ESCs in mammals, yet the biological role of Shp2 in NSC activities and brain development has not been clearly defined.

In this study, we demonstrate that Shp2 is an important player during mammalian brain development, by generating a novel mutant mouse model with Shp2 selectively deleted in neural precursor cells. The conditional Shp2 knockout mice exhibited growth retardation and early postnatal lethality. We demonstrate functional requirements for Shp2 in self-renewing proliferation of NSCs and neuronal and glial cell fate decisions. Our results provide a fresh view of molecular signaling mechanisms coordinating NSC self-renewal and cell lineage specification.

MATERIALS AND METHODS

Animals. Mice were maintained at the Burnham Institute animal facility in accordance with NIH guidelines and approved by the Burnham Institute animal research committee. Generation of a conditional *Shp2* mutant allele (*Shp2*^{flox}) was reported previously (40). Generation and characterization of *nestin-Cre1* and *nestin-Cre2* transgenic mice were described elsewhere (16, 34a).

Primary cortical tissue culture. Cerebral cortices were removed from embryonic day 16.5 (E16.5) and P1 mice, and primary cortical neurons were prepared by trypsinization and mechanical dissociation as previously described (7). Glial cells were removed by preplating the isolated cortical cells suspended in Dul-

* Corresponding author. Mailing address: Burnham Institute for Medical Research, 10901 N. Torrey Pines Rd., La Jolla, CA 92037. Phone: (858) 795-5265. Fax: (858) 713-6274. E-mail: gfeng@burnham.org.

‡ Y.K., E.E.Z., and K.H. made equal contributions to this study.

† Supplemental material for this article may be found at http://mcb.asm.org/.

▽ Published ahead of print on 23 July 2007.

becco's modified Eagle's medium supplemented with 10% fetal calf serum on uncoated culture plates. Neurons recovered as nonadherent cells were allowed to attach on poly-D-lysine- or poly-DL-ornithine- plus laminin-coated cover glasses or culture dishes. The medium was replaced by B27 (Gibco) in neurobasal medium (Gibco), and the cultures were incubated in 10% O_2–5% CO_2 at 37°C. The neurons were incubated in neurobasal medium without B27 for 4 h before growth factor stimulation (brain-derived neurotrophic factor, 10 ng/ml; bFGF, 20 ng/ml; EGF, 20 ng/ml). Astrocytes and oligodendrocytes were cultured as previously described (23).

Immunohistochemistry, immunoblotting and in situ hybridization. The mice were anesthetized with Avertin, perfused with PBS followed by 4% formaldehyde in phosphate-buffered saline. The brain was removed, dehydrated, paraffin sectioned, or cryostat sectioned. Incubation of primary and secondary antibodies was performed following standard protocols. The primary antibodies used were rabbit anti-Shp2 polyclonal from Santa Cruz Biotechnology; mouse anti-nestin monoclonal from the Rat 401 Hybridoma Bank; mouse anti-TuJ1 monoclonal from BABCO; rabbit anti-glial fibrillary acidic protein (GFAP) polyclonal, mouse anti-MAP-2 monoclonal, and mouse anti-O4 monoclonal from Sigma; mouse anti-2′,3′-cyclic nucleotide 3′-phosphodiesterase monoclonal and rabbit anti-NG2 antibody from Chemicon; mouse anti-phosphorylated histone H3 (pH3) polyclonal from Upstate; anti-Ki67 polyclonal from Novo Castra; rabbit anti-cleaved caspase 3 antibody and rabbit anti-Dab1 antibody from Cell Signaling; rabbit anti-p35 antibody from Santa Cruz biotechnology; and rabbit anti-calbindin antibody from Cell Signaling. Preparation of cell/tissue lysates and immunoblot analysis with ECL enhanced chemiluminescence detection were performed following standard protocols and the manufacturer's instructions. The primary antibodies used were mouse anti-beta actin monoclonal antibody from Sigma; rabbit anti-phospho-Erk polyclonal antibody, rabbit anti-phospho-Dab1, rabbit anti-phospho-Stat3(Tyr705) polyclonal antibody, rabbit anti-Stat3 polyclonal antibody, rabbit anti-phospho-C/EBP beta polyclonal antibody, rabbit anti-C/EBP polyclonal antibody, anti-phospho-c-Myc, and anti-c-Myc from Cell Signaling; and anti-Bmi-1 from Upstate Cell Signaling Solutions. RNA in situ hybridization was performed following a protocol previously described (1). The EphA4 probe was a gift from K. Murai (McGill University).

NSC culture and neurosphere assay. Cerebral cortices were dissected from E14.5 embryos and dissociated into single cells. Single cells were suspended and maintained in B27/neurobasal medium supplemented with bFGF (20 ng/ml), EGF (20 ng/ml), and heparin (25 μg/ml). The neurosphere assay was performed to determine self-renewal capacity in NSCs (22). Briefly, spheres were dissociated into a single-cell suspension and reseeded in a 96-well plate at low density (5,000 cells/ml, 200 μl per well). The number and size of secondary or tertiary spheres were determined after 7 days. Neurospheres were counted under an optical microscope, with a minimum cutoff of 40 μm in diameter. A minimum of 12 wells (1,000 single cells seeded per well originally) were counted, and the diameter of at least 10 randomly chosen neurospheres was determined using SimplePCI Advanced Image Capture (AIC) software. MEK inhibitor PD98059 (Cell Signaling), c-Myc inhibitor 10058-F4 (Calbiochem), and Shp2 inhibitor (Wu et al., unpublished data) were used at concentration of 25 μM in 0.05% dimethyl sulfoxide (DMSO), and Stat3 inhibitor AG490 (Calbiochem) was used at concentration of 5 μM in 0.01% DMSO.

Neuronal and astroglial differentiation. NSCs derived from E14.5 embryos or neurospheres were seeded at 20,000 cells/ml onto coverslips precoated with poly-D-lysine (0.1 mg/ml) and laminin (20 μg/ml) in serum-free B27/neurobasal medium with no growth factors. Cells were incubated in adhesion cultures for 5 days to allow neuronal differentiation. Addition of 2% fetal bovine serum on day 5 enhanced neuronal differentiation, and astroglial differentiation was examined 2 days later (on day 7).

Cell proliferation assays. Cell proliferation was assayed by a bromodeoxyuridine (BrdU) detection kit (Roche). BrdU was added to the culture medium (final concentration, 10 μM) and incubated for the desired time periods. Cells were fixed on coverslips and immunostained with a monoclonal anti-BrdU antibody followed by anti-mouse immunoglobulin-fluorescein. Coverslips were mounted in VECTASHIELD mounting medium with DAPI (4′,6′-diamidino-2-phenylindole [staining blue]). $BrdU^+$ cells (fluorescein isothiocyanate) and all cells (blue) were counted under a fluorescent microscope, and at least 10 fields were randomly chosen for counting. The cell growth curve was measured using the real-time cell electronic sensing (RT-CES) system (ACEABIO) (17). Briefly, primary NSCs were diluted and seeded at 10^4 cells/ml on laminin–poly-D-lysine-precoated ACEA 96X microtiter plates in 200 μl of neurobasal/B27 medium. Cell proliferation was monitored in real time by the RT-CES system for a period of 120 h, and the growth curve was analyzed with the RE-CES 2.5 software.

Exogenous Bmi-1 expression. Retroviral expression vector MSCV-Bmi-1-EGFP (for enhanced green fluorescent protein) was kindly provided by S. Morrison (22). Purified vector was cotransfected with pVSVG into GP2-293 packaging cells. The retroviral vehicles were concentrated and added to dissociated primary NSC culture in the presence of 6 μg/ml Polybrene. The number and size of secondary neurospheres were assessed 5 days after viral infection.

RESULTS

Deletion of Shp2 in NSCs leads to early postnatal lethality. In previous experiments, we cloned the murine *Shp2* (previously called *Syp*) cDNA, using a unique PCR strategy designed to search SH2-containing tyrosine phosphatases (9). In situ hybridization detected *Shp2* expression in the neural ectoderm and nervous system in mouse embryos at E9.5 and later stages, suggesting an involvement of Shp2 in neural development (9). To gain insights into the Shp2 function during brain development, we have analyzed *Shp2* expression profiles in the central nervous system. As shown in Fig. S1A in the supplemental material, immunoblotting with a specific anti-Shp2 antibody detected Shp2 protein in isolated neural stem cells, neurons, and astrocytes. Widespread expression of Shp2 was observed in various parts of the adult brain, including the pituitary gland, olfactory bulb, cerebral cortex, hippocampus, cerebellum, and brain stem (see Fig. S1B in the supplemental material).

To decipher Shp2 functions in CNS development, we generated mutant mice with Shp2 selectively deleted in NSCs by crossing a conditional *Shp2* mutant ($Shp2^{F/F}$) mouse line (40), with *nestin-Cre* transgenic mice. We used two different transgenic lines of *nestin-Cre* mice, dubbed as *nestin-Cre1* and *nestin-Cre2*, originally created in the laboratories of Klein and Kageyama, respectively (16, 34a). Crossing of *nestin-Cre1* mice with a *Rosa26lacZ-loxP* reporter mouse line shows efficient and widespread DNA recombination mediated by the Cre recombinase in precursors of neurons and glia starting around E10.5 (34a). The Cre recombinase activity in *nestin-Cre1* mice was detected within the developing cortical wall, and in all cortical layers in postnatal animals, albeit absent in the blood vessels and meninges. In *nestin-Cre2* mice, *Cre* expression was detected in the ventricular zone (VZ) of telencephalon and spinal cord of the developing CNS and also in the dorsal root ganglia when examined at E11.5 (16).

Homozygous mutant pups ($Shp2^{F/F}$::*nestin-Cre*/+, abbreviated as $Shp2^{F/F}$::*Cre*) were born at Mendelian frequency for both mouse lines as genotyped at postnatal day 0 (P0) ($n = 31$ out of 124 pups for $Shp2^{F/F}$::*Cre1* and $n = 28$ out of 105 pups for $Shp2^{F/F}$::*Cre2*, from the crossing of $Shp2^{F/+}$::*Cre*/+ *X* $Shp2^{F/F}$ mice), suggesting no embryonic lethality. Whole-brain lysates of homozygous, heterozygous, and wild-type control mice were analyzed by immunoblotting for Shp2 protein expression. As illustrated in Fig. 1A, Shp2 protein contents were reduced by approximately 90% in brain lysates of both $Shp2^{F/F}$::*Cre1* and $Shp2^{F/F}$::*Cre2* mice at P0 and P4, respectively. The residual 10% of Shp2 protein is likely due to its expression in blood vessels and meninges of the brain, where Cre-mediated DNA recombination did not occur in these two mouse lines, as reported previously (16, 34a).

Notably, both of the mutant mouse lines exhibited a very similar early postnatal lethality phenotype, with the $Shp2^{F/F}$::*Cre1* mice slightly more severely affected than the $Shp2^{F/F}$::*Cre2* animals (Fig. 1B). Most $Shp2^{F/F}$::*Cre1* animals died at P0 to P4, while a few $Shp2^{F/F}$::*Cre2* mice lived a little

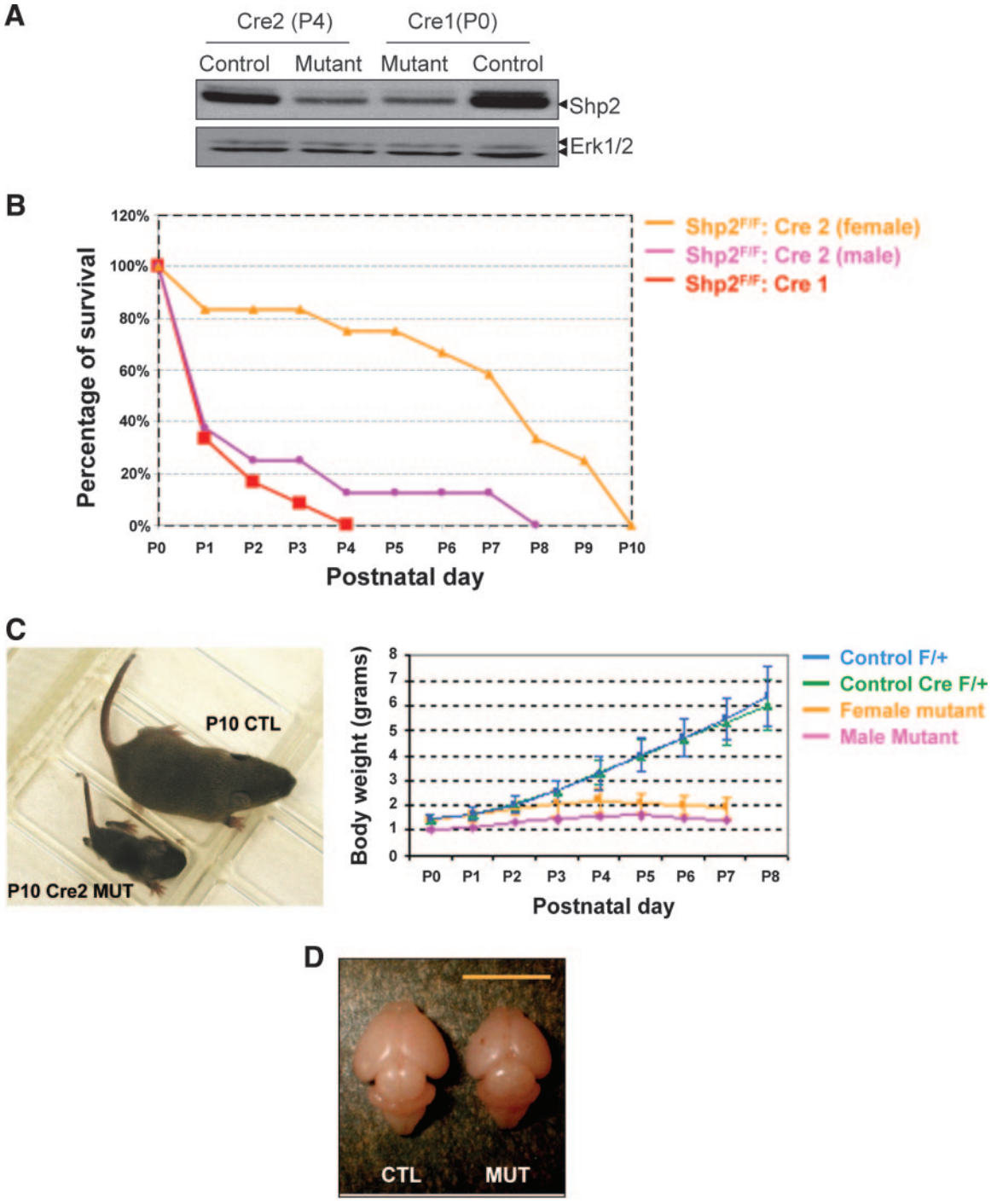

FIG. 1. Deletion of Shp2 leads to early postnatal lethality. (A) Immunoblot analysis of Shp2 protein contents in whole-brain lysates from the control and mutant animals ($Shp2^{F/+}$::Cre2/+ at P4 and $Shp2^{F/F}$::Cre1/+ at P0), with anti-Erk1/2 blotting as loading control. (B) Early postnatal lethality of mutant mice: *Shp2*$^{F/F}$::*Cre1* mutants [red, $n = 12$ (males plus females)], male *Shp2*$^{F/F}$::*Cre2* mutants (pink; $n = 8$) and female *Shp2*$^{F/F}$::*Cre2* mutants (orange; $n = 12$). (C) Growth retardation of surviving *Shp2*$^{F/F}$::*Cre2* mutant mice. (Left panel) One representative pair of littermates at P10. (Right panel) Growth curve. *F*/*F*::*Cre*/+, male, pink; female, orange; *F*/+::*Cre*/+, green; and *F*/+::+/+, blue. (D) Whole brain from control (CTL) and *Shp2*$^{F/F}$::*Cre2* mutant (MUT) at P4.

longer, up to P10. All the surviving *Shp2*$^{F/F}$::*Cre2* mice exhibited a decrease in body weight starting at P4 (Fig. 1C). The growth retardation and postnatal lethality phenotype also appeared gender related, with male mice more severely affected than the females by the *Shp2* mutation. The brain size of mutant mice was reduced when examined at P4 (Fig. 1D). In addition to loss of body weight, we observed development of abnormal behaviors in surviving pups after P4, particularly

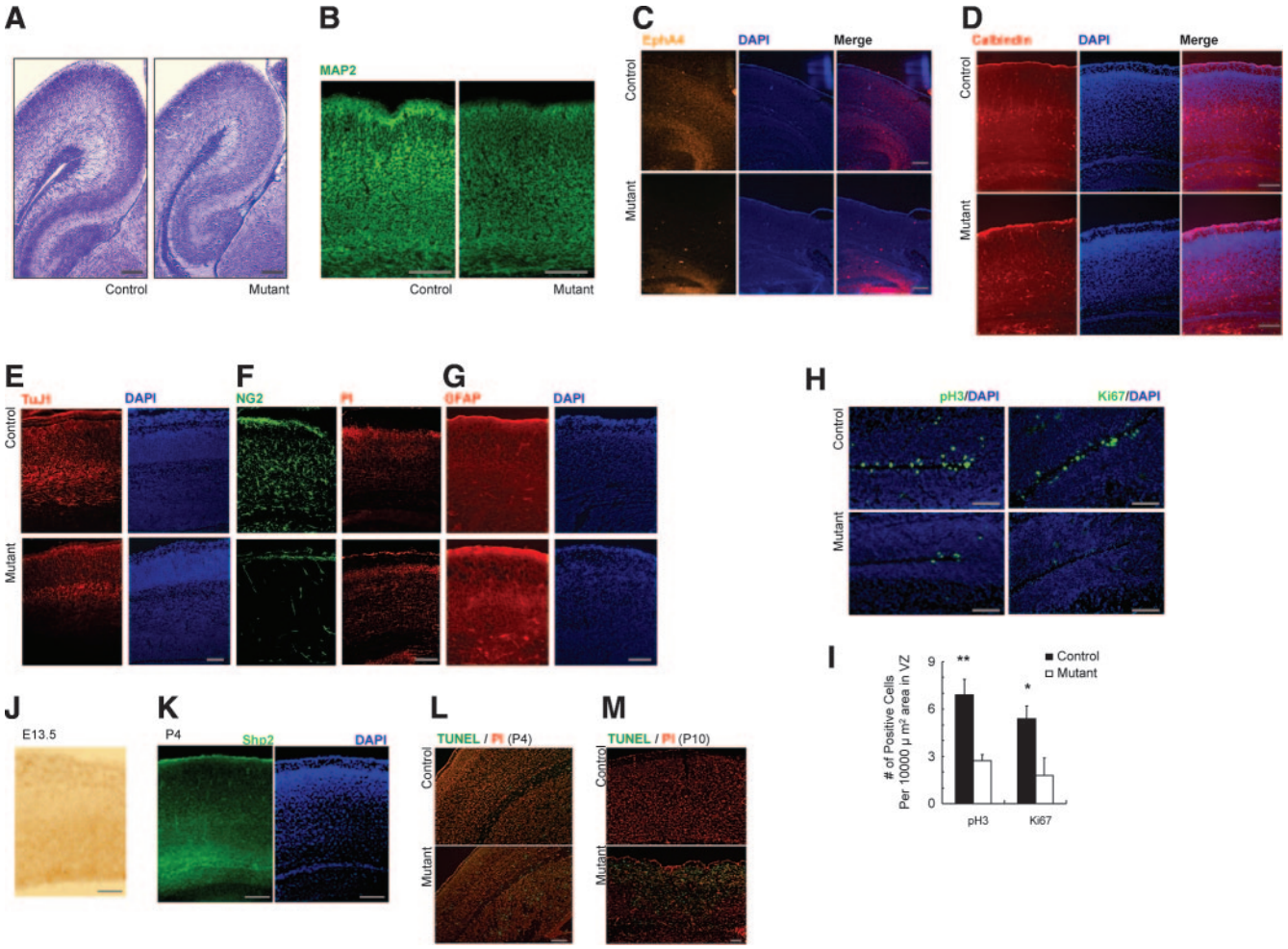

FIG. 2. Impaired corticogenesis. (A) Hematoxylin-and-eosin staining of cerebral cortex at P4. Scale bar, 100 μm. (B) MAP2 expression at P0. Scale bar, 100 μm. (C) EphA4 expression at P0 was examined using in situ hybridization. Scale bar, 100 μm. (D) Calbindin immunostaining at P4. Scale bar, 100 μm. (E to G) Immunostaining for expression of TuJ1 (E) and GFAP (G) in cerebral cortex (E16.5) and NG2 (F) in cerebral cortex (P0). Scale bar, 100 μm. (H) Immunostaining for expression of pH 3 and Ki67 in VZ (E17.5). (I) Significantly reduced numbers of pH 3^+ and $Ki67^+$ cells were detected in the Shp2 mutant VZ (pH3, **, $P < 0.01$; $n = 6\sim7$; Ki67, *, $P < 0.05$; $n = 3$; mutant versus control; scale bar, 100 μm). (J and K) Shp2 expression in VZ at E13.5 (J) and subventricular zone at P4 (K). Scale bar, 100 μm. (L and M) Cell apoptosis by TUNEL assay at P4 (L) and P10 (M). Scale bar, 100 μm. PI, propidium iodide.

ataxia and the inability to suck milk. Multiple factors are likely to contribute to the early postnatal lethality phenotype.

Shp2 has a positive role in corticogenesis. We did not observe a dramatic structural abnormality in the mutant brain. More detailed hematoxylin-and-eosin staining, however, showed that lamination of the cortex was compromised in Shp2-deficient brain (Fig. 2A). We therefore examined cortical development and neuronal cell differentiation/migration using a variety of molecular markers. First, we investigated the expression of MAP2, a marker for dendrite-extended differentiated neurons. High levels of MAP2 expression were detected in the marginal zone and layer V in the control sections at P0, but the signals were weakened in the mutant (Fig. 2B). This result suggests a possibly delayed and impaired neuronal differentiation.

Next, we checked *EphA4* mRNA expression, a marker for layers II and III (Fig. 2C). As compared to controls at P0, almost no signal was detected in the mutant neocortex, which also implies a defective neuronal differentiation because *EphA4* is expressed in postsynaptic regions. Another molecular marker, calbindin, is mainly expressed in layers III and IV. The staining was disorganized in the mutants, showing diffused layers III and IV (Fig. 2D). We also examined expression of *reelin*, a marker of Cajal-Retzius cells in layer I, and found no significant difference in localization and expression levels between wild-type controls and mutants (see Fig. S2A in the supplemental material). No difference in Dab1 (E15.5) and p35 (P0) expression was recognized between controls and mutants (see Fig. S2B and C in the supplemental material). We also treated cortical neurons isolated at E16.5 with Reelin in vitro and checked phosphorylation of Dab1 at Tyr185 and Tyr220. No significant difference was detected between controls and mutants (see Fig. S2D in the supplemental material). Together, these results suggest that ablationof Shp2 had influenced neuronal differentiation but not Reelin-induced cell migration during cortical development.

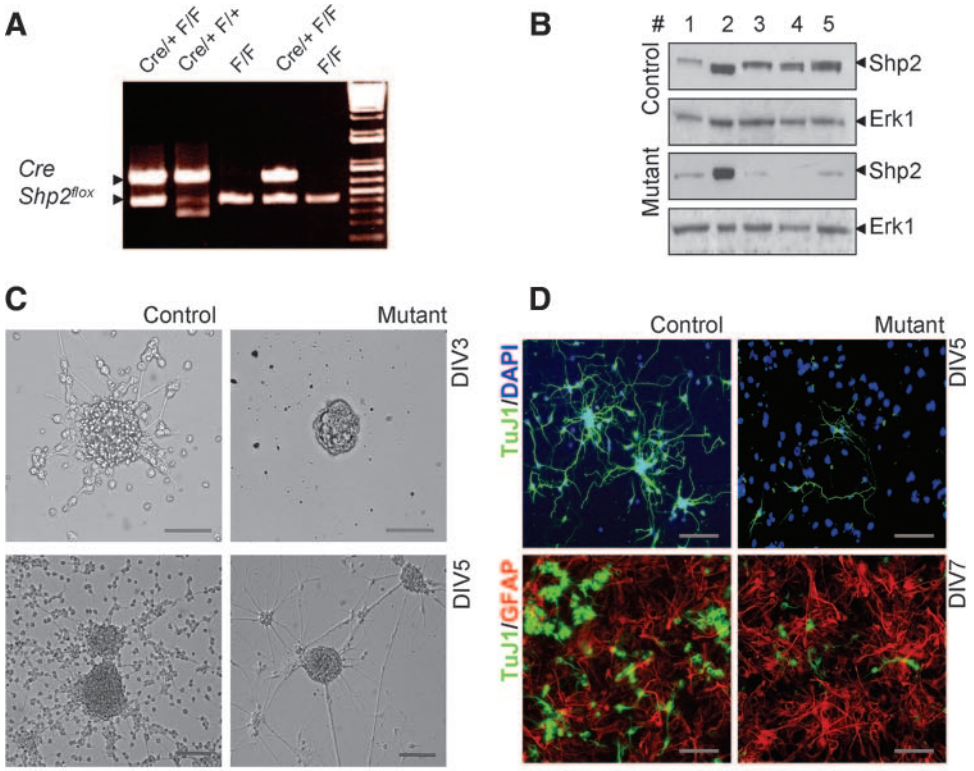

E Generation of Various Neural Cell Lineages

		DIV5	DIV7	DIV10
Neurons (%)	Control	17.4 ± 1.6	16.3 ± 3.5	10.2 ± 1.8
	Mutant	3.1 ± 0.7 **	4.8 ± 1.2 **	5.4 ± 1.6 *
Astrocytes (%)	Control	63.2 ± 3.8	73.7 ± 3.4	84.6 ± 1.4
	Mutant	81.6 ± 4.1 *	82.5 ± 3.0	87.4 ± 1.7
Oligodendrocytes (%)	Control	2.0 ± 1.0	4.2 ± 1.6	2.9 ± 0.4
	Mutant	2.6 ± 1.4	1.3 ± 0.1	0.67 ± 0.03 *

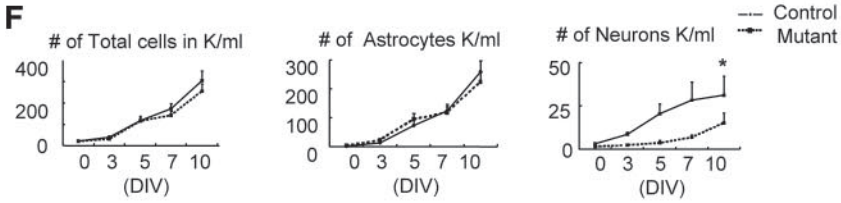

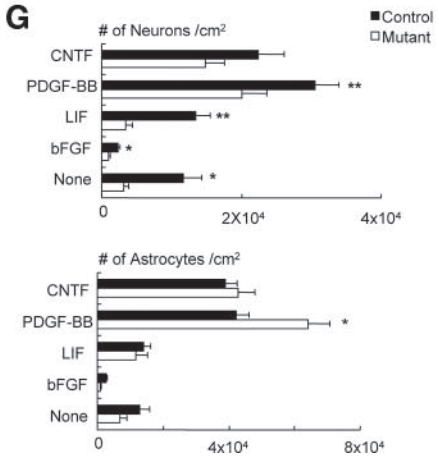

To further investigate the impact of Shp2 deletion on corticogenesis, we examined expression of several cell-type-specific markers in cerebral cortex. Compared to controls, we detected reduced expression levels of neuronal marker (TuJ1) (Fig. 2E) and oligodendrocyte precursor marker (NG2) in the mutant brain (Fig. 2F). In contrast, signals for astrocyte marker protein GFAP were enhanced at E16.5 (Fig. 2G). These observations suggest a defective neurogenesis and oligodendrogenesis in cerebral cortex of the Shp2-deficient brain, while at the expense of neurogenesis, astrogliogenesis appeared slightly enhanced.

Finally, we examined levels of pH3, a marker for metaphase, and Ki67, a proliferative maker, in the VZ of embryonic brain. As shown in Fig. 2H and I, both pH3 and Ki67 signals were significantly decreased in the mutants in comparison to the control, suggesting impaired proliferation of Shp2-deficient NSCs in the mutant VZ. Consistent to this observation, we detected high levels of Shp2 expression in the ventricular zone at E13.5 and subventricular zone at P4 (Fig. 2J and K) in wild-type brain. We also examined the impact of Shp2 deletion on neuronal survival. The terminal deoxynucleotidyltransferase-mediated dUTP-biotin nick end labeling (TUNEL) assay detected increasing levels of cell apoptosis in P4 and P10 mutant cerebral cortex (Fig. 2L and M). Together, these results suggest that Shp2 promotes progenitor proliferation in corticogenesis.

Shp2 oppositely regulates neurogenesis and astrogliogenesis in vitro. The high-level Shp2 expression in the VZ suggests important roles of Shp2 in neural progenitor cells. To further investigate Shp2 function in NSC differentiation and multipotency, we isolated NSCs from cerebral cortex at E14.5 and cultured them in the presence of bFGF and EGF in vitro. NSCs were genotyped to identify Shp2 mutant (*Shp2*$^{flox/flox}$::*Cre*/+) and control (*Shp2*$^{flox/flox}$) cells by PCR analysis of genomic DNA (Fig. 3A). Immunoblotting analysis indicated efficient Cre-mediated deletion of Shp2 in cultured NSCs in vitro (Fig. 3B).

Morphological examination indicated dramatically decreased neurite outgrowth in differentiating neurosphere cultures (Fig. 3C). To precisely evaluate the differentiation capacity, we dissociated the differentiated neurosphere cells and counted numbers of each cell type generated following immunostaining with markers for neurons (TuJ1), astrocytes (GFAP), and oligodendrocytes (O4 or CNPase) at different time points. Analysis of the proportions of TuJ1$^+$, GFAP$^+$, O4$^+$, or CNPase$^+$ cells at days in vitro (DIV) 5, 7, and 10 indicated that Shp2 deficiency severely suppressed neuron and oligodendrocyte differentiation (Fig. 3D and E), consistent with the in vivo results as described above. In contrast, we observed a modest increase in the proportion of astrocytes generated from Shp2-deficient NSCs compared to controls (Fig. 3D and E). However, the absolute numbers of GFAP$^+$ cells were similar between control and Shp2 mutant cultures (Fig. 3F), apparently due to the reduced proliferative capacity of Shp2-deficent progenitor cells under the culture condition.

We further examined neurogenesis and gliogenesis from NSCs following treatment with growth factors or cytokines in vitro. As shown in Fig. 3G, there was a significant decrease in the number of neurons from Shp2-deficient NSCs following stimulation with platelet-derived growth factor (PDGF)-BB, leukemia inhibitory factor (LIF), or bFGF. In response to CNTF, Shp2 deficiency resulted in modestly decreased numbers of neurons ($P > 0.05$; $n = 12$). However, Shp2 ablation did not suppress gliogenesis in response to CNTF, LIF, or bFGF, and there was a significant increase in the number of GFAP$^+$ cells following PDGF-BB treatment ($P < 0.05$; $n = 12$). Collectively, our observations reveal a critical role for Shp2 in neurogenesis and oligodendrogenesis but not in astrogliogenesis. This indicates a cell-type-specific requirement for Shp2 in neural development. The opposite effect of Shp2 deletion on neurogenesis and astrogliogenesis also suggests Shp2 actions in cell fate specification from multipotential progenitor cells.

Shp2 is required for proliferation of NSCs and neuronal progenitors in vitro. We further investigated a putative role of Shp2 in NSC's self-renewal and proliferation potential in vitro. As depicted in Fig. 4A, differences in the number and diameter of neurospheres derived from control and Shp2$^{-/-}$ mutant NSCs were easily observed under a microscope. To further determine the impact of Shp2 deletion on self-renewal of NSCs, we assayed secondary and tertiary neurosphere formation efficiency. As shown in Fig. 4B, Shp2-deficient NSCs exhibited a markedly decreased capacity to generate neurospheres following serial subcloning, suggesting impaired proliferation and/or self-renewal. Indeed, the self-renewal capacity, defined as the number of secondary neurospheres formed per primary neurosphere, was significantly reduced in Shp2$^{-/-}$ NSCs compared to controls. Thus, Shp2 is required for self-renewal of NSCs in vitro (Fig. 4C).

To determine the proliferative capacity, we measured

FIG. 3. Shp2 deficiency results in impaired neurogenesis but modestly enhanced astrogliogenesis. (A) PCR genotyping of the *Shp2*^{F} allele and the *Nestin-Cre* transgene. (B) Immunoblot analysis of tissue or cell lysates. Lane 1, freshly isolated cerebral cortex tissue at E14.5; lane 2, embryonic heart at E14.5; lanes 3, 4, and 5, NSC cultures collected at days 5, 7, and 14. (C) Representative images show reduced neural outgrowth and excessive fasciculation of neurites from Shp2-deficient neurospheres at days 3 and 5 (DIV3 and DIV5), compared to controls. Scale bar, 50 μm. (D) Immunostaining of differentiated cells in culture for TuJ1/DAPI and TuJ1/GFAP. Representative images indicate impaired neurogenesis (TuJ1$^+$) at DIV5 (upper panel) but slightly increased proportion of astrogliogenesis (GFAP$^+$) at DIV7 (lower panel) from Shp2-deficient NSCs. Scale bar, 100 μm. (E) Relative proportions of neurons, astrocytes, and oligodendrocytes were determined by counting TuJ1$^+$, GFAP$^+$, and O4$^+$, or CNPase$^+$ cells, respectively, on DIV 5, 7, and 10 and compared with the total number of cells (**, $P < 0.01$; *, $P < 0.05$; $n = 5$). (F) Decreased numbers of TuJ1$^+$ neurons differentiated from Shp2-deficient NSCs compared to controls (*, $P < 0.05$; $n = 5$). (G) NSC differentiation in response to various growth factors. NSCs were cultured at 2×10^4 cells/ml in neurobasal/B27 serum-free medium, with a daily supplement of CNTF (100 ng/ml), PDGF-BB(100 ng/ml), LIF (3,000 U/ml), or bFGF (20 ng/ml) or with no supplement. Differentiated cells were detected by immunostaining for TuJ1 and GFAP at day 5. Shp2 deficiency resulted in reduced number of neurons following stimulation with PDGF, LIF, and bFGF (**, $P < 0.01$; *, $P < 0.05$; $n = 5$) but caused a significantly increase in the number of astrocytes following PDGF-BB treatment (*, $P < 0.05$; $n = 12$).

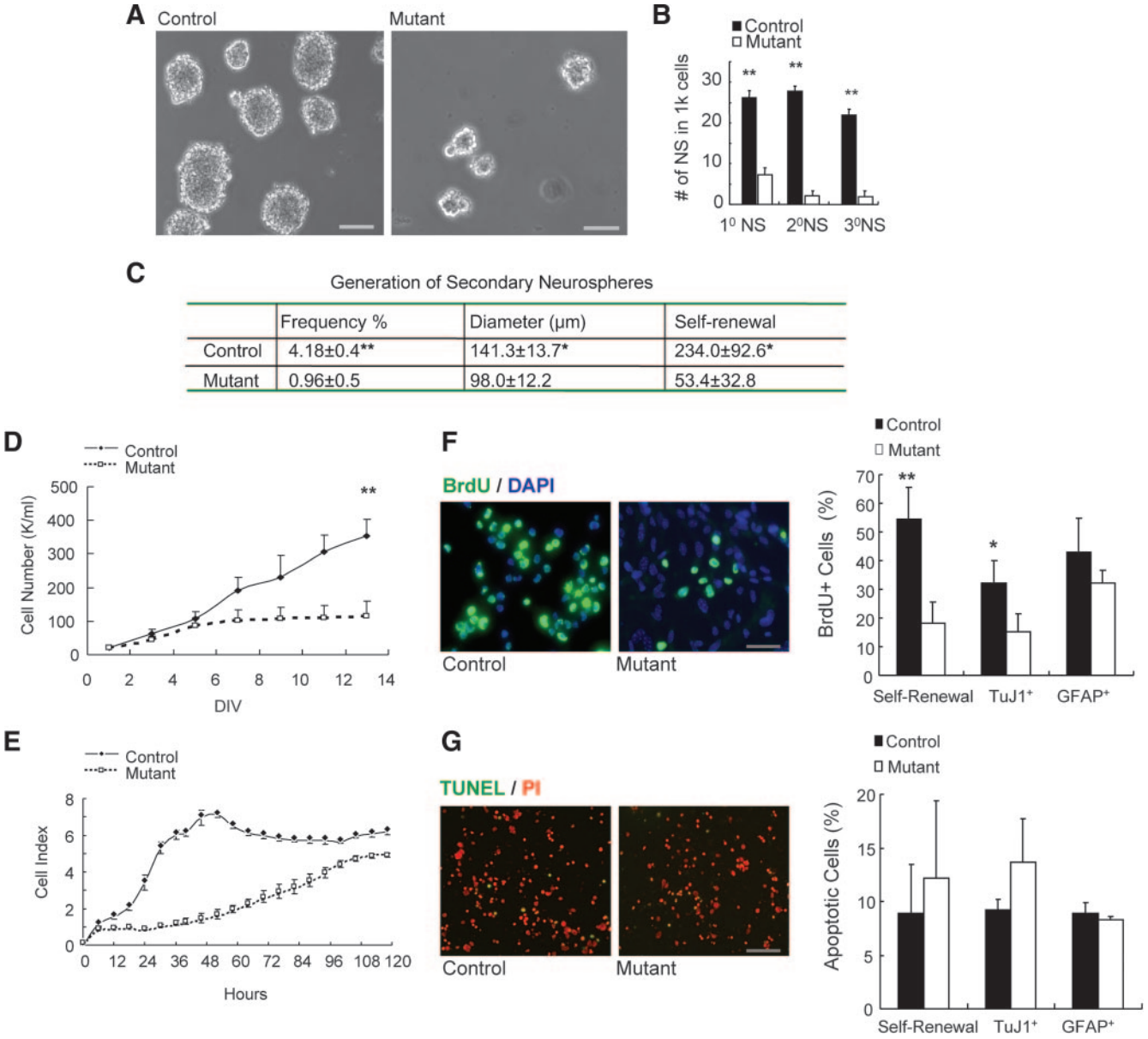

FIG. 4. Shp2 is required for NSC proliferation and self-renewal in vitro. (A) Morphological examination shows the reduced number and size of Shp2 mutant neurospheres as compared to controls. Scale bar, 100 μm. (B) Neurosphere assay. NSCs were initially seeded at 5 cells/μl, and the number of neurospheres (NS) was determined after 7 days for primary (1^0), secondary (2^0), and tertiary (3^0) neurospheres (**, $P < 0.01$; $n = 3$). 1k, 1,000. (C) Generation of secondary neurospheres. The frequency was expressed as the percentage of secondary neurospheres generated versus the total number of single cells dissociated from primary neurospheres. Self-renewal capacity was defined as the number of secondary neurospheres formed per primary neurosphere (*, $P < 0.05$; **, $P < 0.01$; $n = 4$). (D) Growth curve of NSCs in self-renewal culture. Neurospheres in suspension were gently dissociated into single cells and then enumerated (**, $P < 0.01$; $n = 3$). K, 1,000. (E) Growth curve of NSCs in differentiation culture. Single NSCs were seeded on a precoated plate in the absence of bFGF and EGF to induce neuronal differentiation; 2% FBS was added after 24 h to induce astroglial differentiation. Cell proliferation was monitored using the RT-CES system (17). (F) BrdU incorporation assay in NSCs ($Nestin^+$), neurons ($TuJ1^+$ or $MAP2^+$), and astrocytes ($GFAP^+$). (Left panel) Representative pictures of $BrdU^+$ cells in NSCs. (Right panel) Statistical analysis. Scale bar, 50 μm. NSCs: mutant, 18.1% ± 7.5%; control, 54.4% ± 11.2%; **, $P < 0.01$; $n = 5$. Neurons: mutant, 15.3% ± 6.1%; control, 32.5% ± 7.1%; *, $P < 0.05$; $n = 3$. Astrocytes: mutant, 32.3% ± 4.2%; control, 43% ± 12%; $P > 0.05$; $n = 3$). (G) Cell apoptosis (TUNEL) assay in NSCs ($Nestin^+$), neurons ($TuJ1^+$ or $MAP2^+$), and astrocytes ($GFAP^+$). (Left panel) Representative pictures of apoptotic cells in NSCs. Scale bar, 100 μm. (Right panel) Statistical analysis. NSCs: mutant, 12.2% ± 7.2%; control, 8.9% ± 4.6%; $P > 0.05$; $n = 5$. Neurons: mutant, 13.7% ± 4%; control, 9.2% ± 1; *, $P > 0.05$; $n = 3$. Astrocytes: mutant, 8.3% ± 0.3%; control, 8.9% ± 1%; $P > 0.05$; $n = 3$.

growth curves of NSCs under culture conditions that favor either self-renewal or differentiation. When compared to controls, $Shp2^{-/-}$ NSCs exhibited a significantly decreased cell proliferation rate under culture conditions favoring self-renewal expansion (Fig. 4D). Similar proliferative defects of $Shp2^{-/-}$ NSCs were also observed when the stem and progenitor cells were cultured under conditions allowing differentiation into neuronal and astroglial cell lineages (Fig. 4E). To

corroborate these results, we measured BrdU incorporation into cultured neurosphere cells under both self-renewal and differentiation conditions. Consistently, results presented in Fig. 4F show that Shp2 deficiency resulted in significantly reduced proliferation in NSCs and neuronal progenitors ($TuJ1^+$) but not in astroglial cells ($GFAP^+$). Modestly increased levels of cell apoptosis were also detected for Shp2-deficient NSCs and neuronal progenitors compared to wild-type control cells (Fig. 4G). Taken together, these results indicate a primary effect of Shp2 deletion on cell proliferation in self-renewing NSCs and neuronal progenitors.

Shp2 promotes growth factor signals in NSCs. Our previous experiments indicate that despite a decreased proliferation rate, Shp2-deficient mouse ESCs exhibit enhanced self-renewal capacity, as reflected by the increased frequency of secondary embryonic body formation (4, 27). This is in contrast to the observation of impaired self-renewal of Shp2-deficient NSCs as described above. To analyze the molecular basis for distinct functions of Shp2 in ESCs and NSCs, we conducted a comparative analysis of intracellular signaling between these two stem cell types in maintenance cultures (Fig. 5A). We observed remarkably reduced levels of phospho-Erk1/2 in Shp2-deficient NSCs compared to wild-type controls, but no significant difference was detected between wild-type and Shp2 mutant ESCs. Shp2 deficiency resulted in increased phospho-Stat3 levels in both ESCs and NSCs and significantly decreased phospho-Akt in ESCs but not in NSCs. We also found that the phospho-C/EBP signal was significantly decreased in Shp2-deficient NSCs but not in ESCs. Together, these data suggest cell type-specific regulation of signaling pathways by Shp2, which could account for distinct phenotypes seen between Shp2-deficient ESCs and NSCs.

We then explored the possible involvement of Shp2 in relay of signals triggered by specific growth factors in NSCs. As previously reported, there are at least two cell populations in neurospheres—bFGF responsive and EGF dependent NSCs—and both growth factors synergize to promote proliferation (5, 35, 37). Thus, we examined the impact of Shp2 deletion on NSC responses to bFGF and/or EGF. Shp2 deficiency had a modest inhibitory effect on the number and size of neurospheres generated in the presence of EGF alone (Fig. 5B). However, a significantly decreased number and size of neurospheres were detected in Shp2-deficient NSCs, as compared to controls, in response to bFGF alone or bFGF plus EGF (Fig. 5B). This result indicates a primary role of Shp2 in bFGF-dependent NSC proliferation and self-renewal. bFGF has been shown to maintain NSCs by promoting proliferation and suppressing differentiation in vitro and in vivo (26, 32, 34). Stimulation of NSCs by bFGF leads to rapid activation of Erk, whose suppression blocks proliferation of neural progenitors (19). We observed that phospho-Erk signals were much lower in Shp2-deficient NSCs than in controls in response to bFGF (Fig. 5A), suggesting inhibition of bFGF-stimulated Erk activation by Shp2 ablation in NSCs.

To further analyze alterations of bFGF signaling in Shp2-deficient NSCs, we assessed phosphorylation and concomitant activation of c-Myc and Stat3 in response to bFGF. Strikingly, we found opposite activities of Shp2 in modulating c-Myc and Stat3 signaling: Shp2-deficient NSCs exhibited decreased phosphorylation of c-Myc (Thr58/Ser62) but increased phosphorylation of Stat3 (Tyr705) in response to bFGF stimulation (Fig. 5C). Enhanced Stat3 signaling appeared to be specific to bFGF stimulation, as LIF treatment induced similar levels of phospho-Stat3 in control and Shp2-deficient NSCs (Fig. 5C). Augmented bFGF/Stat3 signaling may explain the impaired neurogenesis and moderately enhanced astrogliogenesis in Shp2-deficient NSCs, consistent with the literature (2, 15).

We also took a chemical biology approach to evaluate the effects of Erk, c-Myc, and Stat3 activities in NSCs' self-renewal and neuronal/astroglial differentiation. NSCs were treated with a pharmacological MEK inhibitor (PD98059) and c-Myc inhibitor (10058-F4) and were evaluated for self-renewal in neurosphere assay. As shown in Fig. 5D, treatment with Erk or c-Myc inhibitors resulted in a significantly reduced number of secondary neurospheres, indicating decreased self-renewal capacity. We also treated NSCs with PD98059, 10058-F4, and Jak2/Stat3 inhibitor (AG490) and subjected the cells to neuronal/astroglial differentiation. As depicted in Fig. 5E and F, the MEK inhibitor suppressed neuronal differentiation, whereas c-Myc inhibition had no effect. The Stat3 inhibitor significantly attenuated astroglial differentiation (Fig. 5E and G). In addition, an Shp2 inhibitor recently identified in this laboratory (Wu et al., unpublished data) significantly suppressed self-renewal and neuronal differentiation of NSCs (Fig. 5E and F), consistent with the Shp2 gene knockout data.

The reduced phospho-c-Myc signal also prompted us to examine the expression level of Bmi-1, a transcription factor required for proliferation and self-renewal of NSCs (22), as a recent report suggests that c-Myc directly regulates *Bmi-1* expression (13). Immunoblot analysis showed that consistent with the decreased c-Myc activity, Bmi-1 levels were significantly decreased in Shp2-deficient NSCs compared to controls (Fig. 6A). To define the significance of decreased Bmi-1 expression, we performed a rescue experiment by infecting Shp2-deficient NSCs with a retroviral vector expressing Bmi-1 (Fig. 6B). As indicated in Fig. 6C to E, ectopic expression of Bmi-1 in Shp2-deficient NSCs resulted in increased numbers and size of secondary neurospheres. This result suggests that Shp2 mediates growth factor signals, at least in part via control of Bmi-1 expression, in regulation of NSC proliferation and self-renewal.

DISCUSSION

In this study, we generated and characterized mutant mouse strains with an intracellular tyrosine phosphatase Shp2 selectively deleted in neural precursor cells mediated by *nestin*-driven *Cre* expression. We observed a dramatic phenotype of growth retardation, early postnatal lethality, and multiple defects in proliferation and cell fate specification in NSCs. Of note, we generated the conditional Shp2 knockout mice by using two *nestin-Cre* transgenic mouse lines independently created in two different laboratories, and consistent phenotypes were observed between $Shp2^{F/F}$::*Cre1* and $Shp2^{F/F}$::*Cre2* mice, which renders strength and confidence to the data reported here. In previous studies, we have shown that conditional deletion of Shp2 in postnatal forebrain neurons leads to early onset obesity and leptin resistance (40). Thus, it appears that the same molecule has different jobs/duties at different stages of life. Shp2 modulates NSC activities for brain development at

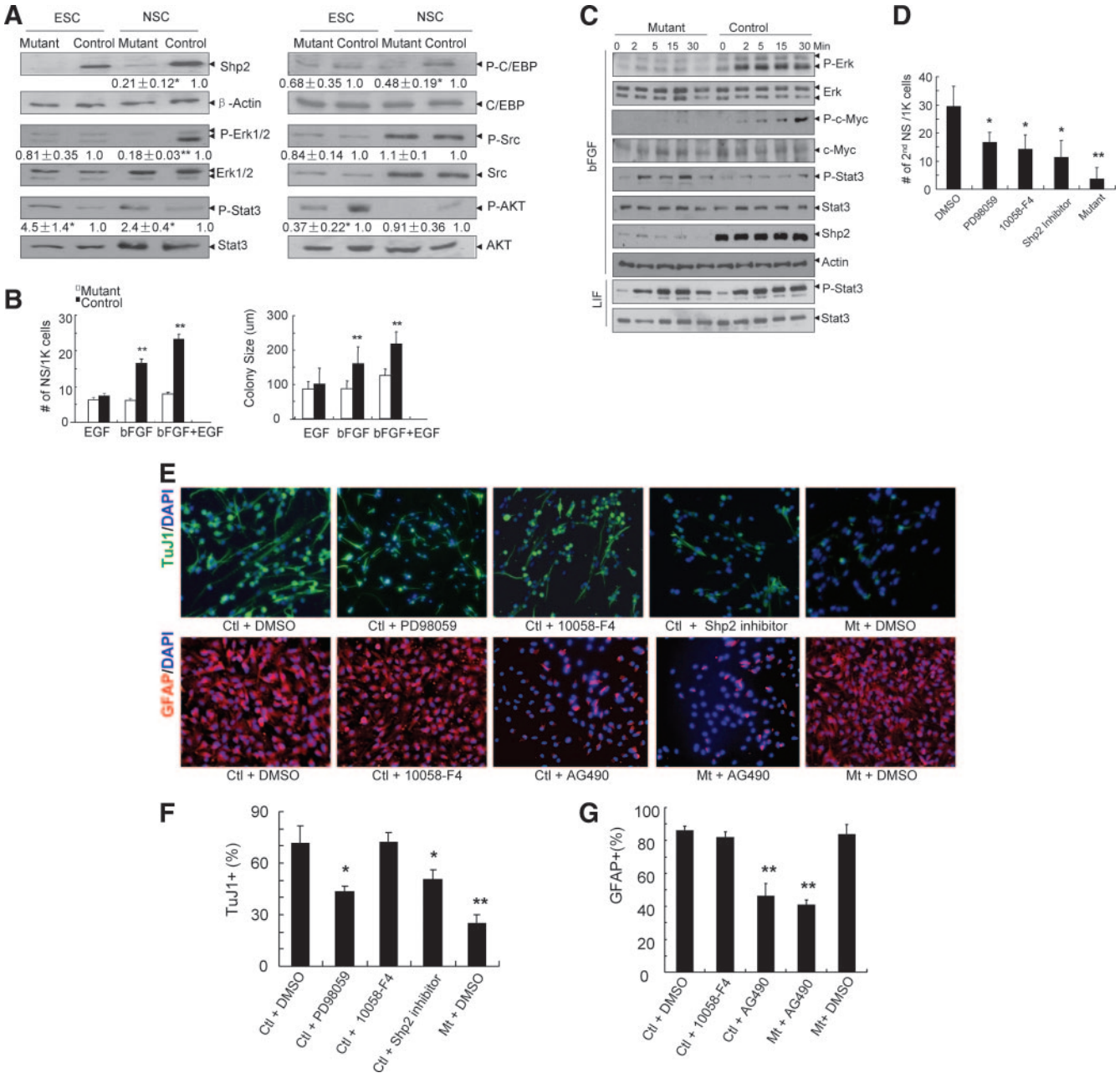

FIG. 5. Shp2 relays growth factor signals in NSCs. (A) Signaling in ESCs and NSCs. Cell lysates were prepared from ESCs and NSCs cultured in the presence of LIF (1,000 U/ml) and bFGF (20 ng/ml), respectively, and immunoblotted for Shp2, β-actin, p-AKT and AKT, p-C/EBP and C/EBP, p-Src and Src, p-Erk and Erk, and pY-Stat3 and Stat3. Band densities (means ± standard errors) are shown for the relative changes (fold) by setting the control level to 1 ($n = 3$ to ~6). **, $P < 0.01$, $n = 6$; *, $P < 0.05$, $n = 3$; mutant versus control. (B) Growth factor signaling. Significant differences were detected in the number (left) and colony size (right) of neurospheres (NS) in response to bFGF or bFGF plus EGF. **, $P < 0.01$; $n = 5$~12; mutant versus control). K, 1,000. (C) bFGF signaling. NSCs were starved and stimulated with bFGF (100 ng/ml) or LIF (1,000 U/ml) for the indicated time periods. Cell lysates were immunoblotted for p-Erk and Erk, p-c-Myc, pY-Stat3 and Stat3, and Shp2 and β-actin. (D) Effects of chemical inhibitors on formation of neurospheres. NSCs in neurosphere cultures were dissociated and seeded at low cell density (1,000 cells/well) with bFGF and EGF plus DMSO (0.05%), PD98059 (25 μM), 10058-F4 (25 μM), or Shp2 inhibitor (25 μM), and neurospheres were enumerated at DIV7. (E) Effects of chemical inhibitors on neuronal/astroglial differentiation. (Upper panel) NSC differentiation under treatment with DMSO (0.05%), PD98059 (25 μM), 10058-F4 (25 μM), or Shp2 inhibitor (25 μM) was assessed by immunostaining with TuJ1 and DAPI at DIV2. (Lower panel) NSC differentiation under treatment with DMSO (0.05%), 10058-F4 (25 μM), and AG490 (5 μM) was evaluated by immunostaining for GFAP and DAPI at DIV4. (F and G) Quantitative analysis of $TuJ1^+$ (F) and $GFAP^+$ (G) cells differentiated under treatment with inhibitors as indicated in panel E. For the percentage of $TuJ1^+$ cells (F), compared to control (Ctl) NSCs with DMSO, a significantly reduced proportion was observed for PD98059 or Shp2 inhibitor (*, $P < 0.05$; $n = 6$) and mutants (Mt) with DMSO (**, $P < 0.01$; $n = 6$). For the percentage of $GFAP^+$ cells (G) compared to control NSCs with DMSO, there was significantly reduced $GFAP^+$ cells in control cells and the mutant with AG490 treatment (both **, $P < 0.01$; $n = 6$).

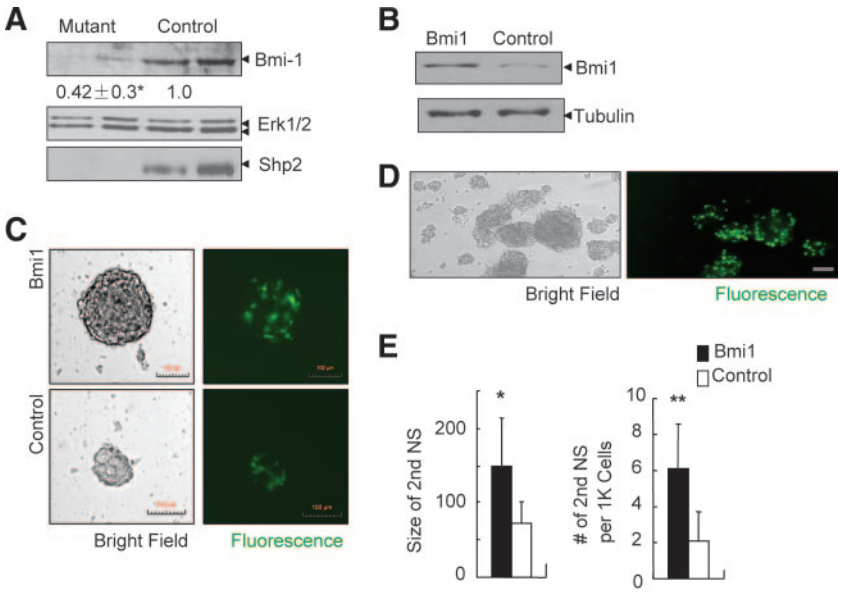

FIG. 6. Exogenous expression of Bmi-1 partially rescues Shp2 deficiency in NSCs. (A) Immunoblot analysis of Bmi-1 expression levels with anti-Erk serving as loading control. Cell genotyping was reconfirmed by anti-Shp2 immunoblotting. Quantitative data were provided after scanning of band density (*, $P < 0.05$; $n = 8$). (B) Exogenous expression of Bmi-1 as determined by immunoblot analysis. Shp2$^{-/-}$ NSCs were infected with MSCV–Bmi-1–EGFP (Bmi1) or control MSCV-EGFP vector (control). (C) Shp2$^{-/-}$ NSCs infected with MSCV–Bmi-1–EGFP exhibited an increased size of neurospheres, compared to that infected with the MSCV-EGFP control virus. Representative pictures were taken 7 days after retroviral infection (scale bar, 100 μm). (D) Enhanced proliferation of Shp2$^{-/-}$ NSCs infected with Bmi-1-expressing retrovirus (EGFP^{+}). Representative pictures were taken 5 days after infection. (E) Shp2$^{-/-}$ NSCs expressing exogenous Bmi-1 exhibited increased size and number of secondary neurospheres (NS). 1K, 1,000. *, $P < 0.05$; $n = 10$; **, $P < 0.01$; $n = 3$.

the early stage, and after completion of brain development, it acts in neuronal control of energy balance and metabolism. Using the conditional Shp2 mutant allele, we are now in a good position to generate other types of neuronal cell-type-specific Shp2 knockout mice and further dissect Shp2 functions in a distinct group of neurons in the brain for understanding of neural development, functions, and neurodegenerative diseases.

This study identifies unique intracellular signaling events underlying control of NSC activities. Shp2 is specifically required for NSC differentiation into neurons and oligodendrocytes but had a negative effect on astroglial differentiation. In mediating neurogenesis and astrogliogenesis, Shp2 appears to modulate Erk and Stat3 pathways in opposite directions. This result suggests that Shp2 participates in cell fate decisions of NSCs during brain development. After submission of the manuscript for this article, we noticed a paper by Gauthier et al. reporting a similar effect of Shp2 tyrosine phosphatase in neuronal/astroglial cell fate decision observed by knockdown of Shp2 expression using the small interfering RNA approach (10).

A common phenotype of Shp2-deficient ESCs and NSCs is reduced proliferative capacity. However, a striking difference is that ESCs lacking functional Shp2 exhibit enhanced self-renewal (4, 27), whereas this study presents data indicating that NSCs require Shp2 for self-renewal. This paradoxical effect of Shp2 ablation on self-renewal of two types of stem cells is apparently due to cell-type-specific modulation of signaling events by Shp2. Several factors likely contribute to these different phenotypes. Shp2 deficiency in ESCs leads to reduced proliferation to a lesser extent than that observed in NSCs. More importantly, Shp2 deficiency results in a drastically decreased differentiation capacity of ESCs, leading to increased self-renewal. In contrast, Shp2 ablation in NSCs potently suppresses proliferation to the point that self-renewal is not possible. In support of this hypothesis, we observed that inhibition of Erk activation is more severe in Shp2$^{-/-}$ NSCs than in Shp2$^{-/-}$ ESCs. Also, enhanced activation of Stat3 in Shp2-deficient ESCs leads primarily to increased self-renewal (24), while a major effect of augmented Stat3 signaling in NSCs is potentiated astrogliogenesis (15), which may also contribute to reduced self-renewal capacity. Further investigation of Shp2 functions in embryonic and adult stem cells should define the molecular machinery functioning in the switch between self-renewal and differentiation of various stem cell types.

Interestingly, we detected a predominant effect of Shp2 in mediating bFGF signaling in NSCs. bFGF is an indispensable trophic factor that permits NSC proliferation and neural development. Mice lacking bFGF have dramatically decreased numbers of neurons and a smaller cortex (6, 36). bFGF activates the Erk pathway mainly by promoting the association of FRS2a (fibroblast receptor substrate 2a) with Shp2 (14). FRS2a knockin mice (Frs2a$^{2F/2F}$) lacking the two Shp2-docking sites display severely impaired cortical development and neurogenesis, due in part to defects in intermediate progenitor cells (38). Interestingly, Frs2α$^{2F/2F}$ NSCs form smaller neurospheres but can self-renew in vitro, in contrast to our observation of Shp2-deficient NSCs' failure in self-renewal in vitro. Therefore, Shp2 may mediate bFGF-stimulated and FRS2 127 -independent signals in NSCs. Deficiency of Shp2$^{-/-}$ NSC self-renewal may also be due to inhibition of unidentified signaling pathways.

Our experiments further suggest that Shp2 deficiency leads to defective growth factor signaling—particularly impaired Erk activation—resulting in reduced activation of transcription factors such as c-Myc and also lower expression levels of Bmi-1. Decreased Bmi-1 expression linked to reduced c-Myc activation in $Shp2^{-/-}$ NSCs is consistent with the recently published data suggesting control of *Bmi-1* expression by c-Myc (13). Therefore, we propose that a bFGF/Shp2/Erk/c-Myc/Bmi-1 pathway is essential for NSC self-renewal. Support for this theory is our result that exogenous expression of Bmi-1 partially rescued the phenotype induced by Shp2 deficiency in NSCs. Bmi-1 promotes neural stem cell proliferation by repressing cyclin-dependent kinase inhibitors such as $p16^{INK4a}$ or $p19^{INK4d}$ (3, 21, 22). Bmi-1 has also been shown to be required for proliferation and self-renewal of leukemic and hematopoietic stem cells in addition to neural stem cells (19, 25, 31). Given that Shp2 also plays an essential role in regulating hematopoiesis and HSC activities, it is very likely that a common signaling pathway involving Shp2 and Bmi-1 operates in the self-renewal of both hematopoietic and neural stem cells. Nevertheless, it is conceivable that Shp2 acting in signaling events proximal to specific growth factor receptors may have multiple effects in signaling pathways. Accordingly, we have noted a difference in the phenotypes of Shp2-deficient and Bmi-1-deficient NSCs. Although both Shp2 and Bmi-1 are essential for NSC self-renewal and both inhibit astrogliogenesis, Bmi-1 deficiency has no significant effect on neurogenesis (22, 39), while loss of Shp2 leads to defective neurogenesis as reported here. Bmi-1-deficient mice survive into adulthood and show developmental retardation (22). However, Shp2 mutant mice die in the uterus (33), and mice with Shp2 selectively deleted in the brain exhibit early postnatal lethality, indicating that Shp2 has more extensive physiological effects than Bmi-1. Identification of pathways altered in Shp2-deficient NSCs should further define the molecular basis for the control of NSC self-renewal and multipotentiality.

ACKNOWLEDGMENTS

This work was supported by NIH grants R01CA78606 and R01GM53660 and a pilot project of P20GM075059 to G.S.F. Y.P. is a recipient of a postdoctoral fellowship from the California Institute of Regenerative Medicine, and Y.K. received a postdoctoral fellowship from the California Breast Cancer Research Program.

We thank S. Morrison, K. Murai, J. de Castro and W. B. Stallcup for reagents and valuable suggestions and Feng laboratory members for helpful discussion.

REFERENCES

1. **Albrecht, U., H.-C. Lu, J.-P. Revelli, X.-C. Xu, R. Lotan, and G. Eichele.** 1998. Studying gene expression on tissue sections using *in situ* hybridization, p. 93–120. *In* K. W. Adolph (ed.), Human genome methods. CRC Press, Inc., Boca Raton, FL.
2. **Bonni, A., Y. Sun, M. Nadal-Vicens, A. Bhatt, D. A. Frank, I. Rozovsky, N. Stahl, G. D. Yancopoulos, and M. E. Greenberg.** 1997. Regulation of gliogenesis in the central nervous system by the JAK-STAT signaling pathway. Science **278:**477–483.
3. **Bruggeman, S. W., M. E. Valk-Lingbeek, P. P. van der Stoop, J. J. Jacobs, K. Kieboom, E. Tanger, D. Hulsman, C. Leung, Y. Arsenijevic, S. Marino, and M. van Lohuizen.** 2005. Ink4a and Arf differentially affect cell proliferation and neural stem cell self-renewal in Bmi1-deficient mice. Genes Dev. **19:**1438–1443.
4. **Chan, R. J., S. A. Johnson, Y. Li, M. C. Yoder, and G. S. Feng.** 2003. A definitive role of Shp-2 tyrosine phosphatase in mediating embryonic stem cell differentiation and hematopoiesis. Blood **102:**2074–2080.
5. **Ciccolini, F., and C. N. Svendsen.** 1998. Fibroblast growth factor 2 (FGF-2) promotes acquisition of epidermal growth factor (EGF) responsiveness in mouse striatal precursor cells: identification of neural precursors responding to both EGF and FGF-2. J. Neurosci. **18:**7869–7880.
6. **Dono, R., G. Texido, R. Dussel, H. Ehmke, and R. Zeller.** 1998. Impaired cerebral cortex development and blood pressure regulation in FGF-2-deficient mice. EMBO J. **17:**4213–4225.
7. **Ethell, I. M., and Y. Yamaguchi.** 1999. Cell surface heparan sulfate proteoglycan syndecan-2 induces the maturation of dendritic spines in rat hippocampal neurons. J. Cell Biol. **144:**575–586.
8. **Feng, G. S.** 1999. Shp-2 tyrosine phosphatase: signaling one cell or many. Exp. Cell Res. **253:**47–54.
9. **Feng, G. S., C. C. Hui, and T. Pawson.** 1993. SH2-containing phosphotyrosine phosphatase as a target of protein-tyrosine kinases. Science **259:**1607–1611.
10. **Gauthier, A. S., O. Furstoss, T. Araki, R. Chan, B. G. Neel, D. R. Kaplan, and F. D. Miller.** 2007. Control of CNS cell-fate decisions by SHP-2 and its dysregulation in Noonan syndrome. Neuron **54:**245–262.
11. Reference deleted.
12. **Gritti, A., E. A. Parati, L. Cova, P. Frolichsthal, R. Galli, E. Wanke, L. Faravelli, D. J. Morassutti, F. Roisen, D. D. Nickel, and A. L. Vescovi.** 1996. Multipotential stem cells from the adult mouse brain proliferate and self-renew in response to basic fibroblast growth factor. J. Neurosci. **16:**1091–1100.
13. **Guney, I., S. Wu, and J. M. Sedivy.** 2006. Reduced c-Myc signaling triggers telomere-independent senescence by regulating Bmi-1 and p16(INK4a). Proc. Natl. Acad. Sci. USA **103:**3645–3650.
14. **Hadari, Y. R., H. Kouhara, I. Lax, and J. Schlessinger.** 1998. Binding of Shp2 tyrosine phosphatase to FRS2 is essential for fibroblast growth factor-induced PC12 cell differentiation. Mol. Cell. Biol. **18:**3966–3973.
15. **He, F., W. Ge, K. Martinowich, S. Becker-Catania, V. Coskun, W. Zhu, H. Wu, D. Castro, F. Guillemot, G. Fan, J. de Vellis, and Y. E. Sun.** 2005. A positive autoregulatory loop of Jak-STAT signaling controls the onset of astrogliogenesis. Nat. Neurosci. **8:**616–625.
16. **Isaka, F., M. Ishibashi, W. Taki, N. Hashimoto, S. Nakanishi, and R. Kageyama.** 1999. Ectopic expression of the bHLH gene Math1 disturbs neural development. Eur. J. Neurosci. **11:**2582–2588.
17. **Ke, Y., D. Wu, F. Princen, T. Nguyen, Y. Pang, J. Lesperance, W. J. Muller, R. G. Oshima, and G. S. Feng.** 2007. Role of Gab2 in mammary tumorigenesis and metastasis. Oncogene **26:**4951–4960.
18. **Lai, L. A., C. Zhao, E. E. Zhang, and G. S. Feng.** 2004. The Shp-2 tyrosine phosphatase, p. 275–299. *In* J. Arino and D. Alexander (ed.), Protein phosphatases, vol. 5. Springer-Verlag, Berlin, Germany.
19. **Lessard, J., and G. Sauvageau.** 2003. Bmi-1 determines the proliferative capacity of normal and leukaemic stem cells. Nature **423:**255–260.
20. **Menard, C., P. Hein, A. Paquin, A. Savelson, X. M. Yang, D. Lederfein, F. Barnabe-Heider, A. A. Mir, E. Sterneck, A. C. Peterson, P. F. Johnson, C. Vinson, and F. D. Miller.** 2002. An essential role for a MEK-C/EBP pathway during growth factor-regulated cortical neurogenesis. Neuron **36:**597–610.
21. **Molofsky, A. V., S. He, M. Bydon, S. J. Morrison, and R. Pardal.** 2005. Bmi-1 promotes neural stem cell self-renewal and neural development but not mouse growth and survival by repressing the p16Ink4a and p19Arf senescence pathways. Genes Dev. **19:**1432–1437.
22. **Molofsky, A. V., R. Pardal, T. Iwashita, I. K. Park, M. F. Clarke, and S. J. Morrison.** 2003. Bmi-1 dependence distinguishes neural stem cell self-renewal from progenitor proliferation. Nature **425:**962–967.
23. **Nishiyama, A., X. H. Lin, N. Giese, C. H. Heldin, and W. B. Stallcup.** 1996. Interaction between NG2 proteoglycan and PDGF alpha-receptor on O2A progenitor cells is required for optimal response to PDGF. J. Neurosci. Res. **43:**315–330.
24. **Niwa, H., T. Burdon, I. Chambers, and A. Smith.** 1998. Self-renewal of pluripotent embryonic stem cells is mediated via activation of STAT3. Genes Dev. **12:**2048–2060.
25. **Park, I. K., D. Qian, M. Kiel, M. W. Becker, M. Pihalja, I. L. Weissman, S. J. Morrison, and M. F. Clarke.** 2003. Bmi-1 is required for maintenance of adult self-renewing haematopoietic stem cells. Nature **423:**302–305.
26. **Qian, X., A. A. Davis, S. K. Goderie, and S. Temple.** 1997. FGF2 concentration regulates the generation of neurons and glia from multipotent cortical stem cells. Neuron **18:**81–93.
27. **Qu, C. K., and G. S. Feng.** 1998. Shp-2 has a positive regulatory role in ES cell differentiation and proliferation. Oncogene **17:**433–440.
28. **Qu, C. K., S. Nguyen, J. Chen, and G. S. Feng.** 2001. Requirement of Shp-2 tyrosine phosphatase in lymphoid and hematopoietic cell development. Blood **97:**911–914.
29. **Qu, C.-K., W.-M. Yu, B. Azzarelli, S. Cooper, H. E. Broxmeyer, and G.-S. Feng.** 1998. Biased suppression of hematopoiesis and multiple developmental defects in chimeric mice containing Shp-2 mutant cells. Mol. Cell. Biol. **18:**6075–6082.
30. **Qu, C.-K., Z.-Q. Shi, R. Shen, F.-Y. Tsai, S. H. Orkin, and G.-S. Feng.** 1997. A deletion mutation in the SH2-N domain of Shp-2 severely suppresses hematopoietic cell development. Mol. Cell. Biol. **17:**5499–5507.
31. **Raaphorst, F. M.** 2003. Self-renewal of hematopoietic and leukemic stem cells: a central role for the Polycomb-group gene Bmi-1. Trends Immunol. **24:**522–524.

32. **Raballo, R., J. Rhee, R. Lyn-Cook, J. F. Leckman, M. L. Schwartz, and F. M. Vaccarino.** 2000. Basic fibroblast growth factor (Fgf2) is necessary for cell proliferation and neurogenesis in the developing cerebral cortex. J. Neurosci. **20:**5012–5023.
33. **Saxton, T. M., M. Henkemeyer, S. Gasca, R. Shen, D. J. Rossi, F. Shalaby, G. S. Feng, and T. Pawson.** 1997. Abnormal mesoderm patterning in mouse embryos mutant for the SH2 tyrosine phosphatase Shp-2. EMBO J. **16:**2352–2364.
34. **Taupin, P., J. Ray, W. H. Fischer, S. T. Suhr, K. Hakansson, A. Grubb, and F. H. Gage.** 2000. FGF-2-responsive neural stem cell proliferation requires CCg, a novel autocrine/paracrine cofactor. Neuron **28:**385–397.
34a. **Tronche, F., C. Kellendonk, O. Kretz, P. Gass, K. Anlag, P. C. Orban, R. Bock, R. Klein, and G. Schutz.** 1999. Disruption of the glucocorticoid receptor gene in the nervous system results in reduced anxiety. Nat. Genet. **23:**99–103.
35. **Tropepe, V., M. Sibilia, B. G. Ciruna, J. Rossant, E. F. Wagner, and D. van der Kooy.** 1999. Distinct neural stem cells proliferate in response to EGF and FGF in the developing mouse telencephalon. Dev. Biol. **208:**166–188.
36. **Vaccarino, F. M., M. L. Schwartz, R. Raballo, J. Nilsen, J. Rhee, M. Zhou, T. Doetschman, J. D. Coffin, J. J. Wyland, and Y. T. Hung.** 1999. Changes in cerebral cortex size are governed by fibroblast growth factor during embryogenesis. Nat. Neurosci. **2:**848.
37. **Vescovi, A. L., B. A. Reynolds, D. D. Fraser, and S. Weiss.** 1993. bFGF regulates the proliferative fate of unipotent (neuronal) and bipotent (neuronal/astroglial) EGF-generated CNS progenitor cells. Neuron **11:**951–966.
38. **Yamamoto, S., I. Yoshino, T. Shimazaki, M. Murohashi, R. F. Hevner, I. Lax, H. Okano, M. Shibuya, J. Schlessinger, and N. Gotoh.** 2005. Essential role of Shp2-binding sites on FRS2alpha for corticogenesis and for FGF2-dependent proliferation of neural progenitor cells. Proc. Natl. Acad. Sci. USA **102:**15983–15988.
39. **Zencak, D., M. Lingbeek, C. Kostic, M. Tekaya, E. Tanger, D. Hornfeld, M. Jaquet, F. L. Munier, D. F. Schorderet, M. van Lohuizen, and Y. Arsenijevic.** 2005. Bmi1 loss produces an increase in astroglial cells and a decrease in neural stem cell population and proliferation. J. Neurosci. **25:**5774–5783.
40. **Zhang, E. E., E. Chapeau, K. Hagihara, and G. S. Feng.** 2004. Neuronal Shp2 tyrosine phosphatase controls energy balance and metabolism. Proc. Natl. Acad. Sci. USA **101:**16064–16069.